

Gamma flashes from relativistic electron-positron plasma droplets

Munshi G. Mustafa^{1,2,*} and B. Kämpfer^{1,3,†}

¹*Forschungszentrum Dresden-Rossendorf, 01314 Dresden, Germany*

²*Theory Division, Saha Institute of Nuclear Physics, 1/AF Bidhannagar, Kolkata 700064, India*

³*Institut für Theoretische Physik, TU Dresden, 01062 Dresden, Germany*

Ultra-intense lasers are expected to produce, in near future, relativistic electron-positron plasma droplets. Considering the local photon production rate in complete leading order in quantum electrodynamics (QED), we point out that these droplets are interesting sources of gamma ray flashes.

PACS numbers: 12.20.-m, 52.50.Jm, 52.27.Ny, 52.25.Os

Keywords: Quantum electrodynamics, Laser, Relativistic plasma, Gamma radiation and absorption

Fastly progressing high-intensity laser technology [1, 2] offers the perspective to create relativistic plasmas composed of electrons (e^-), positrons (e^+) and photons (γ) under laboratory conditions. Accordingly simulations have been performed, *e.g.*, in [3, 4] for special scenarios. Ideally would be the creation of an equilibrated $e^+e^- \gamma$ plasma of sufficient size exceeding the mean free path of photons. Such a state of matter with properties reviewed in [5] is governed by thermo-field theory applied to QED and also in [6] by kinetic theory. If such a plasma could be produced by table-top laser installations, it would represent the QED pendant to the QCD quark-gluon plasma currently investigated with large-scale accelerators [7]. Relativistic plasmas have some interesting specific features, such as collective plasmon or plasmino excitations [8] with accompanying van Hove singularities [9]. Electron-positron plasmas are also interesting for astrophysical scenario [10]. Temperatures of about $T \sim 10$ MeV, in a laser-generated plasma, would open, furthermore, channels for muon or pion production [11]. While these channels are interesting for their own right (see [12] for another avenue for laser driven particle production), a hot $e^+e^- \gamma$ plasma droplet, exploding after the creation process by the enormous thermodynamic pressure, is a source of γ radiation. Such short γ flashes may be of future use in ultra-fast spectroscopic investigations of various kind.

In this note, we are going to present estimates of the photon spectrum emerging from a $e^+e^- \gamma$ plasma droplet with temperatures in the 10 MeV range. In contrast to often employed particle-in-cell (PIC) simulations (see [3] for a study of the start-up phase of a similarly hot plasma), we base our considerations on results from QED thermo-field theory. The expansion dynamics is treated in a schematic way, as our emphasis is on the photon emission characteristics.

The calculation of the local spontaneous photon emission rate from a QED (electron-positron) plasma has been outlined in [13] to complete leading order in elec-

tromagnetic coupling α by including two-loop order. The result, at the heart of our note, may be presented as

$$\frac{dN}{d^4x d^3E_\gamma} = \frac{2\alpha m_\infty^2 n_F(E_\gamma)}{(2\pi)^3 E_\gamma} \left[\ln\left(\frac{T}{m_\infty}\right) + \frac{1}{2} \ln\left(\frac{2E_\gamma}{T}\right) + C_{22}\left(\frac{E_\gamma}{T}\right) + C_b\left(\frac{E_\gamma}{T}\right) + C_a\left(\frac{E_\gamma}{T}\right) \right] \quad (1)$$

where $n_F(E_\gamma) = (\exp(E_\gamma/T) + 1)^{-1}$ denotes the Fermi distribution, and the dynamically generated asymptotic mass squared of the electron is $m_\infty^2 = 2m_{\text{th}}^2$. The thermal mass squared is given by $m_{\text{th}}^2 = e^2 T^2/8$ with $e^2 = 4\pi\alpha$ (The considerations apply for $T > m_{e^\pm}$ which are different from the non-relativistic case where the relevant scales are given by the masses of plasma particles and the temperature [5].) $E_\gamma = u \cdot k$ is a short hand notation for the Lorentz scalar product of the medium's four-velocity $u(t, \vec{x})$ and the photon's four-momentum k . This rate includes $2 \leftrightarrow 2$ processes from one loop [14], *viz.*, Compton scattering and pair annihilation which generate the leading logarithmic contribution (first three terms in (1)). In addition, the rate also includes the inelastic processes [15] from two-loop like bremsstrahlung (fourth term) and off-shell pair annihilation (fifth term) with the correct incorporation [13, 16] of the Landau-Pomeranchuk-Migdal effect that limits the coherence length of the emitted radiation. A common feature of the latter two processes is that they have off-shell fermion next to the vertex where the photon is emitted, and the virtuality of the fermion becomes very small if the photon is emitted in forward direction. However, contrary to the one-loop diagrams, the singularity is linear instead of logarithmic, and it brings a factor T^2/m_{th}^2 making it the same order in α as that of one-loop. The functions C s are independent of α (because the relative importance of scattering with a photon to an another charged particle in the plasma is essentially given by the ratio m_∞^2/m_D^2 , where m_D is the Debye screening mass) but are nontrivial functions of $y = E_\gamma/T$ determined by a set of integral equations [13, 16]. The numerical results for electron-positron plasma are described quite accurately by phenomenological fits in the domain $0.1 \leq y \leq 30$ which is sufficient for our consideration. The C_{22} is same in QED and QCD

*Electronic address: musnhigolam.mustafa@saha.ac.in

†Electronic address: b.kampfer@fzd.de

because the interference effect cancels out and is given as

$$C_{22}(y) \simeq 0.041y^{-1} - 0.3615 + 1.01e^{-1.35y}, \quad (2)$$

whereas the other two coefficients due to inelastic processes in QED are fitted together yielding

$$C_b(y) + C_a(y) \simeq \frac{2a \ln(b + 1/y)}{y^c} + \frac{2dy}{\sqrt{1 + y/f}}, \quad (3)$$

where $a = 0.374958$, $b = 0.431304$, $c = -0.05465$, $d = 0.157472$ and $f = 1.73085$.

In Fig. 1, the scaled differential photon rate is displayed as a function of scaled photon energy. A comparison reveals that the low-energy photon rate is suppressed in the QED plasma relative to a QCD plasma (consisting of quarks, anti-quarks and gluons, all strongly interacting). The reason is that a photon has a non-negligible medium induced thermal mass, while in QCD its thermal mass is suppressed relative to the quarks by (e^2/g^2) , where g is the strong coupling in QCD.

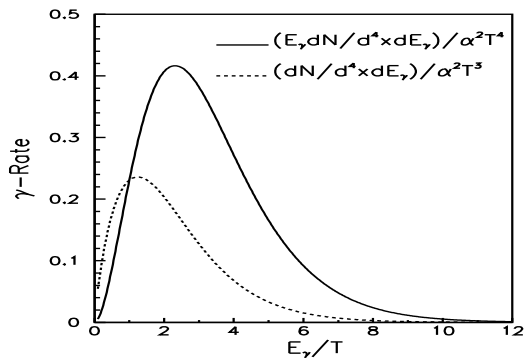


FIG. 1: Differential photon emission rate (dashed) as well that of energy weighted (solid) for an equilibrated, symmetric $e^+e^- \gamma$ plasma as a function of photon energy scaled with temperature.

The damping of a photon is related to the absorption of it in the medium. The damping rate can be obtained from the photon production rate in (1) by the principle of detailed balance [13, 17, 18] as

$$\Gamma_\gamma(E_\gamma) = \frac{(2\pi)^3}{4} e^{E_\gamma/T} \frac{dN}{d^4x d^3E_\gamma}, \quad (4)$$

where the prefactor, $(2\pi)^3/4$, is a matter of definition [18]. The mean free path, λ_γ , of a photon in a medium is inversely related to the photon damping rate as $\lambda_\gamma = 1/\Gamma_\gamma$. In Fig. 2 the mean free paths of photons are displayed as a function of temperature of the electron-positron plasma for a wide range of photon energies. This figure reveals very interesting features of the $e^+e^- \gamma$ plasma droplet. Apparently at initial temperature, it appears to be completely opaque as discussed in Refs. [5, 11]. However, it may not be so forever as we will see below. For a given photon energy E_γ the mean free

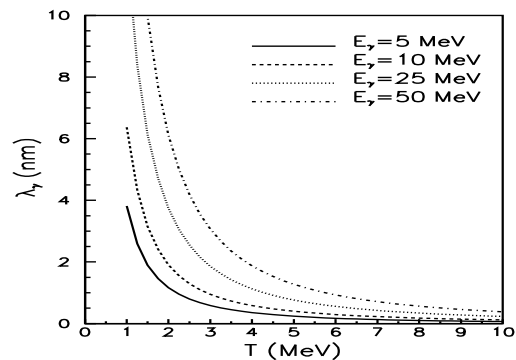


FIG. 2: Mean free path of photons of energy E_γ in an equilibrated, symmetric $e^+e^- \gamma$ plasma as a function of temperature.

path increases with decreasing temperature implying a dilute system after some time. On the other hand, for a given T it increases with energy, E_γ , making the system more transparent to the low energy photons depending upon the size of the plasma droplet. However, the realistic scenario would be to consider the expansion of the droplet due to thermodynamic pressure.

We consider the expansion with spherical geometry of radius $R(t) = R_0 + v(t)t$, where R_0 is the initial size of the droplet, $v(t)$ is the surface velocity of the droplet assumed as $v(t) = \eta t$, where η is a constant having dimension $c^2/[\text{Length}]$. We adopt a linear flow profile $v(t, r) = v(t)r/R(t)$. The space-time integrated radiation spectrum follows from

$$E_\gamma \frac{dN}{dE_\gamma} = 2 \int_0^t dt \int_0^{R(t)} dr r^2 \int_0^{2\pi} d\phi \times \left(E_\gamma \frac{dN}{d^4x dE_\gamma} \right) \Theta[\lambda_\gamma(t) - L(r, \phi)], \quad (5)$$

where $L(r, \phi) = (R^2(t) - r^2 \sin^2 \phi)^{1/2} - r \cos \phi$ is the distance [19] the photon travels after it is created at a point r with an angle ϕ relative to the radial direction. This expression takes into account that the radiation can only be emitted from such positions r and in such directions ϕ where the distances to the surface $R(t)$ is shorter than the mean free path $\lambda_\gamma(t)$. The temperature at a time instant t is calculated by employing the energy conservation relation: $E(t) = E_0 - E_\gamma^{\text{em}}(t) - E^{\text{kin}}(t)$, where E_0 is the initial energy of the droplet obtained from the total initial energy density, $\epsilon(T_0) = 11\pi^2 T_0^4/60 \simeq 3.8 \times 10^{29} \text{ Jm}^{-3}$ at $T_0 = 10 \text{ MeV}$. We note that E_0 ($\propto T_0^4 R_0^3$) depends crucially on the initial droplet size. $E_0 \simeq 13 \text{ kJ}$ for a droplet of radius $R_0 = 2 \text{ nm}$ with the same reasoning as in Ref. [11]. (It is an interesting and challenging topic how the laser pulse energy can be deposited in a smallest possible spatial and temporal volume. The scenario in Ref. [3, 11] envisages, *e.g.*, an initial stage of compressed foil with $(1 - 2) \text{ nm}$ thickness and $T_0 \sim 10 \text{ MeV}$). Now, at any instant of time t , one can obtain the energy of the emitted photon as $E_\gamma^{\text{em}}(t) = \int dE_\gamma (E_\gamma dN/dE_\gamma)$ from

(5), and the kinetic energy of the droplet as $E^{\text{kin}}(t) = 4\pi \int dr r^2 \epsilon(T(t))\gamma v(t, r)$, with $\gamma = 1/(1-v^2(t, r)/c^2)^{1/2}$. The evolution is truncated at time t_f at which T cools down to 1 MeV. For lower temperatures, the electron rest mass becomes a relevant scale which modifies the employed rate. As we are interested in the hard part of the emission spectrum, $E_\gamma \geq 1$ MeV, the late evolution with $T \leq 1$ MeV is not essential for our purposes.

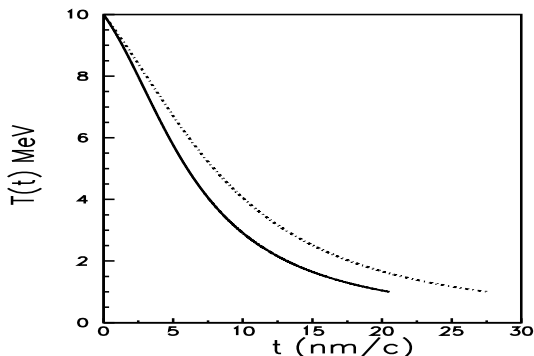


FIG. 3: Temperature as a function of time for $\eta = 0.03 c^2/\text{nm}$ (solid) and $0.01 c^2/\text{nm}$ (dashed).

In Fig. 3, the evolution of $T(t)$ is displayed for two surface velocities. The expansion lasts up to $t_f \sim (20 - 30) \text{ nm}/c$. A realistic three-dimensional expansion dynamics can be obtained from relativistic hydrodynamics from given initial conditions, in particular phase space distribution. This deserves separate dedicated investigations which we postpone. A relevant scale is the velocity of sound ($1/\sqrt{3}$ in an ideal relativistic plasma) at which a rarefaction wave travels from the surface towards the center is compatible with our consideration. We note that the evolution depends strongly on the system size but weakly on the surface expansion velocity.

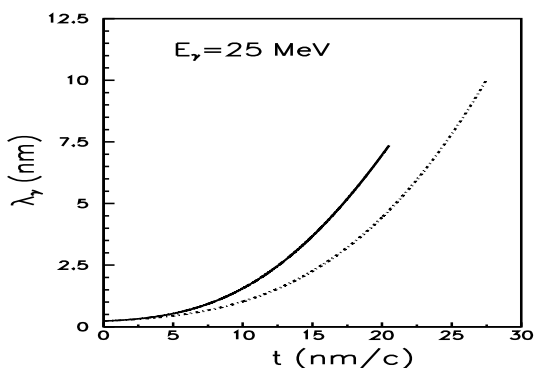


FIG. 4: Mean free path of a photon with $E_\gamma = 25$ MeV as a function of time for $\eta = 0.03 c^2/\text{nm}$ (solid) and $0.01 c^2/\text{nm}$ (dashed).

In Fig. 4, we display the evolution of $\lambda_\gamma(t)$ with same initial conditions as above. The mean free path of the photon for the expanding droplet depends on the velocity profile. This in turn determines the region from which the

photons may escape. The system becomes more dilute and transparent in later time. Inspection of Fig. 2 also unravels that harder photons have a larger optical depth, as mentioned above.

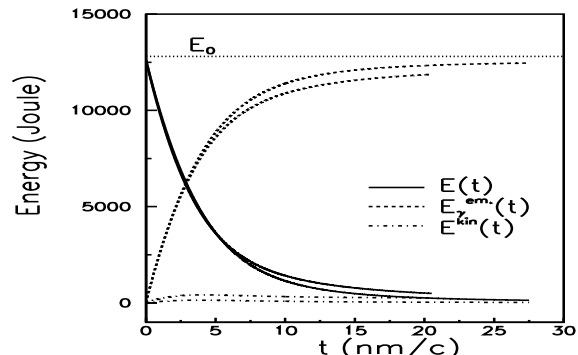


FIG. 5: Evolution of $E(t)$ (solid), $E_\gamma^{\text{em}}(t)$ (dashed) and $E^{\text{kin}}(t)$ (dash-dotted) for $\eta = 0.03 c^2/\text{nm}$ and $0.01 c^2/\text{nm}$. A larger value of t_f corresponds to a smaller value of η .

In Fig. 5, we exhibit the evolution of various energies with same initial conditions as above. Initially, E^{kin} increases with the increase of time but then decreases as the size of the system becomes larger and the local energy density drops. The integrated energy of emitted photons increases with time indicating that the most of the system's energy is attributed to photon production. Thus, the total energy remaining in the droplet decreases with time. The surprising fact is that cooling by photon emission is very efficient, i.e. the initial energy of the plasma droplet is converted essentially into hard photon radiation. This limits the time span the droplet spends in a hot stage. In addition, e^+ and e^- leakage reduces the life time of the hot era further. The droplet, after equilibration, appears a gamma flash. Of course, there are relaxation processes, like heat conductivity etc. The present estimate assumes that these are short compared with the expansion time scale.

In Fig. 6, we display the energy weighted photon spectra. As seen there is an enormous amount of photon production from the electron-positron plasma droplet. Note that the time integrated photon spectrum scales roughly with the initial volume or energy E_0 , respectively. For instance, a one-order change in initial radius would correspond to a three-orders of magnitude change in photon production.

We now briefly discuss an asymmetric plasma with non-zero net electric charge. The chemical potential μ steers such an asymmetry. The ratio of electron to positron densities is approximately $\propto \exp\{2\mu/T\}$, while the net density behaves like $\propto \mu T^2$ in leading order. That means, a noticeable difference in e^+ and e^- densities translates into $\mu \geq T$. μ enters the photon rate in (1) through $m_\infty^2 = e^2 T^2 (1 + \mu^2/(\pi^2 T^2))/4$, which takes into account the number of charge particles available for various processes. Also various C s depend on μ through

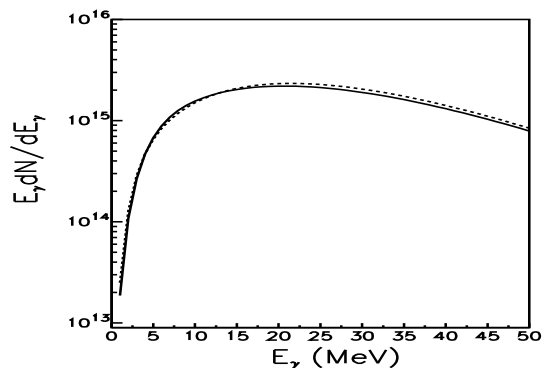


FIG. 6: Energy weighted photon spectrum as a function of photon energy for surface expansion velocities with $\eta = 0.03 c^2/\text{nm}$ (solid) and $0.01 c^2/\text{nm}$ (dashed). Radiation from the ignition stage is not included.

the ratio $m_\infty^2/m_D^2 \sim (1 + \mu^2/(\pi^2 T^2))/(1 + 3\mu^2/(\pi^2 T^2))$ which accounts for, as discussed earlier, the relative importance of scattering with a photon to a charge in the plasma. Therefore, it could only be important at $\mu \geq T$.

The present considerations are armed with a state-of-the-art photon emissivity. The dynamics, in contrast, is rather schematic: constant temperature over the fireball, linear velocity profile, prescribed surface velocity and velocity profile etc. Envisaged calculations within relativistic hydrodynamics including gradients and details of radiation transport will make the scheme more realistic.

Clearly, chemical undersaturation [3, 20] (which would correspond to a decrease of the initial energy density for the same initial temperature) parameterized by fugacities need to be included along the lines of [21] to arrive at a detailed picture. The effect of impurities, like ions or the original material where the plasma is formed from, should be considered too, as other expansion patterns, e.g. for the geometry envisaged in Ref. [3].

In summary we point out that a hot $e^+e^-\gamma$ plasma droplet created by ultra-intense and short laser pulses is a technologically interesting source of γ flashes with continuous spectrum (and not only a flash of 511 keV radiation as argued in Ref. [3]) ranging up to energies being a multitude of the initial temperature. To have an estimate of the efficiency for transforming the incoming eV laser photons into hard gamma radiation, we mention that the integrated power in the γ flash is comparable to the total energy of the initial plasma droplet. Hereby we considered only photons with $E_\gamma \geq 1$ MeV. In the considered scenario, the other energy, after disintegration, resides in collective (radial) flow of electrons and positrons and soft photons.

The authors thank T.E. Cowan and R. Sauerbrey for inspiring debates and G. D. Moore for supplying the numerical results leading to equation (3). MGM would like to acknowledge various useful discussions with M. H. Thoma and Rajarshi Ray. He is also thankful to FZ Dresden-Rossendorf for supporting his stay as a FZD-fellow during the course of this work.

-
- [1] G.A. Mourou, T. Tajima and S.V. Bulanov, *Rev. Mod. Phys.* **78**, 309 (2006); Y.I. Salamin, S.X. Hu, K.Z. Hatsagortsyan and C.H. Keitel, *Phys. Rep.* **427**, 41 (2006).
- [2] *Ultra High Intensity Laser Acceleration of Ions to MeV/Nucleon Energies (2007)*, Particle Accelerator Conference PAC07, 25-29 Jun 2007, Albuquerque, NM.
- [3] B. Shen and J. Meyer-ter-Vehn, *Phys. Rev. E* **65**, 016405 (2001).
- [4] E. P. Liang S. C. Wilks and M. Tabak, *Phys. Rev. Lett.* **81**, 4887 (1998).
- [5] M. H. Thoma, arXiv:0801.0956 (To appear in *Rev. Mod. Phys.*, 2008).
- [6] R. Ruffini, L. Vitagliano and She-S. Xue, *Phys. Lett.* **B559**, 12 (2003).
- [7] *Proceedings of 19th International Conference on Relativistic Heavy-Ion Collisions*; *J. Phys. G: Nucl. Part. Phys.* **34**, 1 (2007).
- [8] M. Le Bellac, *Thermal Field Theory*, *Thermal Field Theory* (Cambridge University Press, 1996); J. I. Kapusta and C. Gale, *Finite-Temperature Field Theory Principles and Applications* (Cambridge University Press, 1996).
- [9] E. Braaten, R. Pisarski and T. C. Yuan, *Phys. Rev. Lett.* **64**, 2242 (1990); M. G. Mustafa, A. Schäfer and M. H. Thoma, *Phys. Rev. C* **61**, 024902 (1999); A. Peshier and M. Thoma, *Phys. Rev. Lett.* **84**, 841 (2000); F. Karsch, M. G. Mustafa and M. H. Thoma, *Phys. Lett.* **B497**, 249 (2001).
- [10] H. Takabe, *Prog. Theor. Phys. Suppl.* **143**, 2002 (2001).
- [11] I. Kuznetsova, D. Habs and J. Rafelski, *Phys. Rev. D* **78**, 014027 (2008).
- [12] B. Henrich and K.Z. Hatsagortsyan, C.H. Keitel, *Phys. Rev. Lett.* **93**, 013601 (2004).
- [13] P. Arnold, G. D. Moore and L. G. Yaffe, *J. High. Energy Phys.* **12**, 009 (2001).
- [14] J. Kapusta, P. Lichard and D. Seibert, *Phys. Rev. D* **44**, 2774 (1991); R. Baier, H. Nakkagawa, A. Niegawa and K. Redlich, *Z. Phys.* **C53**, 433 (1992).
- [15] P. Aurenche, F. Gelis, R. Kobes and H. Zaraket, *Phys. Rev. D* **58**, 085003 (1998).
- [16] P. Arnold, G. D. Moore and L. G. Yaffe, *J. High. Energy Phys.* **11**, 057 (2001).
- [17] H. A. Weldon, *Phys. Rev. D* **28**, 2007 (1983).
- [18] M. H. Thoma, *Phys. Rev. D* **51**, 862 (1995).
- [19] B. Müller, *Phys. Rev. C* **67**, 061901 (2003); M. G. Mustafa and M. H. Thoma, *Acta Phys. Hung. A* **22**, 93 (2005); M. G. Mustafa, *Phys. Rev. C* **72**, 014905 (2005).
- [20] A. G. Aksenov, R. Ruffini and G. V. Vereshchagin, *Phys. Rev. Lett.* **99**, 125003 (2007).
- [21] B. Kämpfer and O.P. Pavlenko, *Z. Phys.* **C62**, 491 (1994); T. S. Biro et al., *Phys. Rev. C* **48**, 1275 (1993); D. K. Srivastava, M. G. Mustafa and B. Müller, *Phys. Rev. C* **56**, 1064 (1997); *Phys. Lett.* **B396**, 45 (1997); M. G. Mustafa and M. H. Thoma, *Phys. Rev. C* **62**, 014902 (2000); *ibid* **63**, 069902 (2001).